doi: 10.32131/jes.4.18

Journal of the Earth Simulator, Volume 4, December 2005, 18–30

Development of an Integrated Earth System Model on the Earth Simulator

Michio Kawamiya[1]*, Chisato Yoshikawa[1], Tomomichi Kato[1], Hisashi Sato[1], Kengo Sudo[1], Shingo Watanabe[1] and Taroh Matsuno[1]

[1] *Frontier Research Center for Global Change, Japan Agency for Marine-Earth Science and Technology, Yokohama, Japan.*

(Received February 8, 2005; Revised manuscript accepted October 18, 2005)

Abstract The project aims at development of an integrated earth system model, where biological and chemical processes important for the global environment are included to interact with climate changes. The model is developed by adding individual component models to atmospheric and oceanic general circulation models (GCMs). The component models are terrestrial and oceanic carbon cycle models and an atmospheric chemistry model. Improvements of the physical climate model are required in order to extend the model top to the middle atmosphere. Preliminary results with fully-coupled climate - carbon cycle model show a significant positive feedback between climate change and carbon cycle, while another preceding model exhibits an even stronger feedback. Experiments with the atmospheric chemistry component model demonstrate that impact of climate change on other green house gases such as tropospheric ozone and methane could be significant. As a first step to improve the atmospheric GCM (AGCM), resolution-dependence of momentum transfer by gravity waves is investigated using high resolution AGCMs which explicitly resolve gravity waves.

Keywords: Earth system, Carbon cycle, Vegetation dynamics, Atmospheric chemistry, Gravity wave

1. Introduction

An integrated earth-system model is being developed at the Frontier Research Center for Global Change (FRCGC) in collaboration with the Center for Climate System Research (CCSR) of the University of Tokyo and the National Institute for Environmental Studies (NIES). The project started October 2002 as a component of the Japan Model Mission of the Kyousei Project and will continue until March 2007.

The objective of the project is to model variations and changes of the global environment as a whole, as an integrated system including physical climatic processes, biogeochemical processes and eco-dynamical processes. Necessity of such modeling is recently appreciated in the context of global warming projection, because climate change caused by emission of CO_2 is supposed to influence the carbon cycle to change significantly terrestrial and oceanic uptakes of CO_2 and hence the atmospheric CO_2 concentration which, in turn, feeds back to climate change [1, 2]. Thus the carbon cycle and climate change should be treated simultaneously including their interactions. In the same way changes of other greenhouse gasses such as CH_4 and O_3 must be treated in the coupled chemistry-climate model. Change of vegetation that may occur following climate change is also a critical factor among many impacts of global warming and must be projected by use of a model as realistic as possible. Furthermore, some phenomena that involve stratospheric processes, such as ozone exchange between the stratosphere and the troposphere, could have a significant impact on surface climate [3]. An ideal earth system model should therefore include land and ocean carbon cycle components with dynamic vegetation, and an atmospheric chemistry component with a sophisticated representation of the stratosphere.

For developing such an integrated model of the global environment, FRCGC has an advantage in that there are research programs to study individual processes and develop models of various subsystems of the global environmental system, such as atmospheric chemistry, terrestrial and oceanic carbon cycles and so forth. Thus our strategy is to couple existing sub-models of biogeochemical and ecological processes to the already working physical climate model which was developed at CCSR, NIES,

* ***Corresponding author***: *Dr. Michio Kawamiya, Frontier Research Center for Global Change, Japan Agency for Marine-Earth Science and Technology, 3173-25, Showamachi, Kanazawa-ku, Yokohama, 236-0001, Japan. E-mail: kawamiya@jamstec.go.jp*

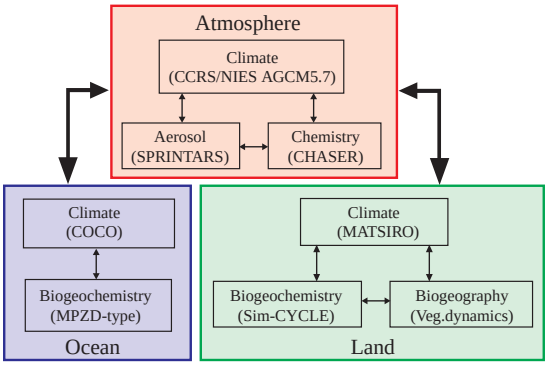

Fig. 1 Structure of the integrated earth system model, Kyousei-2 Integrated Synergetic System Model of the Earth (KISSME). Note that the vegetation dynamics model is now separately developed and yet to be incorporated in KISSME.

and FRCGC. The whole system is code-named "Kyousei-2 Integrated Synergetic System Model of the Earth (KISSME)" (Fig. 1).

As to vegetation dynamics we are developing a new type of model which explicitly simulates individual plants. In what follows the present status of our activities is reported. Section 2 introduces results from the carbon cycle component and provides a brief explanation on the dynamic vegetation model, although it is yet to be run on the Earth Simulator (ES). Section 3 describes the atmospheric chemistry component CHASER, together with some discussion on results obtained by CHASER-only experiments. Attempts to improve the representation of the stratospheric circulation are described in Section 4. Section 5 summarizes this report.

2. Global Carbon Cycle Model

2.1 Description of the model and experiment

The terrestrial carbon cycle model, Sim-CYCLE was originally developed by scientists at the University of Tsukuba [4] and brought in to FRCGC when they joined the project. In the model carbon storage is divided into 5 compartments, that is, leaves, stems, roots, litter or dead biota and soil organic matters, and processes to represent flows among carbon pools including exchanges between the atmosphere and vegetation/soil are included. Biota is classified into 20 types and their geographical distribution is fixed, meaning that change of vegetation types due to climate change is not represented. The model was used in various studies and known to show reasonable behaviors. In the context of the present project, so called off-line calculations on the response of terrestrial carbon storage to some projected future climate changes were performed [5, 6].

The ocean component of the carbon cycle model was newly developed for the present project's objectives. (The pre-existing model at FRCGC is more eco-dynamics oriented and complicated [7].) The ocean GCM and the coupled AOGCM developed at CCSR/NIES/FRCGC are adopted as the base model and ecological/biogeochemical processes have been introduced. As the ecosystem process model a nutrient-phytoplankton-zooplankton-detritus type model [8, 9] was adopted. In addition to this a series of inorganic carbon reactions were introduced following the recommended form by the Ocean Carbon Cycle Model Intercomparison Project (OCMIP).

The physical climate system model in which these carbon cycle components are embedded is the lower resolution version of MIROC, developed by CCSR, NIES, and FRCGC. The atmospheric model has a horizontal resolution of T42, approximately equivalent to 2.8° grid size, and 20 σ-layers in the vertical with relatively fine vertical resolution in the planetary boundary layer. The height of the model top is currently ~30 km. The ocean model has a zonal resolution of 1.4° (= 360/256), and a spatially varying meridional resolution that is about 0.56° at latitudes lower than 8°, 1.4° at latitudes higher than 65°, and smoothly changes in between. The ocean model adopts a hybrid vertical coordinate system; the uppermost 8 levels out of the 43 use the σ-coordinate and the rest the z-coordinate. The model has a bottom boundary layer in addition to the 43 levels. No flux adjustment is applied for the coupling. Further details of the coupled model are provided in a dedicated report [10].

An experiment is carried out to examine the magnitude of positive feedback between global warming and carbon cycle found in preceding works [1, 2]. The spin-up is conducted by running the integrated model for 280 years starting from the initial conditions based on climatological data sets until globally integrated net CO_2 fluxes at land and sea surfaces vanish. Three different runs are performed: the control run in which atmospheric CO_2 concentration is fixed at 285 ppmv throughout the entire integration period after the spin-up, i.e., for 1850-2100; and the other two runs (coupled and uncoupled run), in which the observed time series of the atmospheric CO_2 concentration is given to the model during 1850-1900, and from 1901 to 2100, CO_2 emission data (SRES A2 scenario) are given to the model instead of concentration data. In the coupled run atmospheric CO_2 concentration was allowed to vary as calculated by the carbon cycle components, but in the uncoupled run, the changing CO_2 concentration had no impact on climate because the fixed value of 285 ppmv was used for radiation routines. In the coupled run, on the other hand, CO_2 concentration calculated by the carbon cycle components was used for radiation calculation so that climate change takes place, which in turn affects the carbon cycle.

2.2 Results and discussion

Fig. 2 shows model calculations of CO_2 concentration by the integrated model. It can be seen that the model results agree well with the observed evolution of CO_2 concentration until 2000. There are two lines corresponding to the coupled (red) and the uncoupled (green) run. There is a significant difference between the two experiments, and it is seen that the effect of global warming on carbon cycle is to increase CO_2 in the atmosphere; in other words, it accelerates global warming. This is because decomposition of soil organic carbon is enhanced by the soil temperature rise following the surface temperature rise of 4.0°C projected by this particular model. The strength of positive feedback due to climate – carbon cycle interactions is 130 ppmv in terms of difference in global mean atmospheric CO_2 concentration at 2100 between the coupled and uncoupled runs, while other models show a variety of feedback strength (e.g., 225 ppmv by the Hadley centre model [1], 75 ppmv by the IPSL model [2]). The present results should be seen with some caution because the parameter tuning for the terrestrial carbon cycle component is still underway since the initialized state of land carbon storage of 3100 PgC was larger than typical simulation values of 2100 – 2200 PgC [11, 12], although it is within the range of uncertainty (1746 – 3392 PgC) suggested by an observation-based study [13]. It would certainly deepen our understandings on the global carbon cycle to compare results from various models and identify what causes such differences between models.

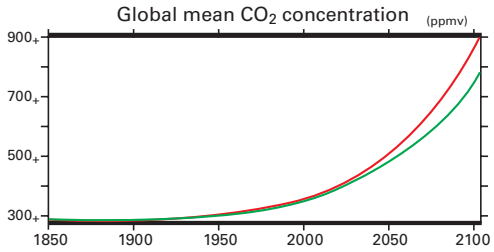

Fig. 2 Development of atmospheric CO_2 concentration obtained by providing CO_2 emission data as model input after 1900. The red line shows the case where interactions between climate and carbon cycle are considered, and the green line not. Units are ppmv.

An international project C4MIP (Coupled Carbon-Cycle Climate Model Inter-comparison Project) has been established in order to facilitate such comparative studies, and discussions made in C4MIP will be reflected in the 4th assessment report of IPCC (Intergovernmental Panel on Climate Change). We regard C4MIP as an important step toward our international contribution, and shall examine our results following a method adopted by C4MIP

An analysis method has been devised to facilitate comparison among different models [14] by dividing the climate – carbon cycle feedback into four elements, that is, land and ocean carbon cycle sensitivity to atmospheric CO_2 (β_{AB} and β_{AO} in Table 1) and land and ocean carbon cycle sensitivity to temperature change (γ_{AB} and γ_{AO}). The method was applied to the results by the Hadley centre [1] and IPSL [2] and the figures displayed in Table 1 were obtained. The table also shows the figures from our present experiment. In this particular experiment, our model yields γ_{AB} and γ_{AO} similar to those by IPSL. The resultant gain factor g, which shows relative increase of atmospheric CO_2 concentration due to the climate – carbon cycle feedback, is thus similar to that of the IPSL model, while the gain factor is slightly higher in the present experiment due to its lower β_{AB} and β_{AO}. Although it is not clear yet what leads to the differences in sensitivities, the impact of the large land carbon storage in the present experiments should be checked when comparisons are made among different models. As pointed out in a previous report [15], release of CO_2 from organic carbon stored on land is a major component for the climate – carbon cycle feedback. It is planned to perform experiments with the present model, whose results will be presented elsewhere, using different parameter sets to examine the model's behaviors with different terrestrial and oceanic carbon stocks.

Table 1 Estimate of the climate – carbon cycle feedback for three simulations

	α	β_{AB}	β_{AO}	γ_{AB}	γ_{AO}	g	f
Hadley	0.0086	1.66	0.94	–201	–26.4	0.41	1.69
IPSL	0.0072	1.675	1.7	–89.8	–36.8	0.166	1.2
FRCGC	0.0070	1.29	1.29	–80.9	–36.3	0.23	1.30

α is the climate sensitivity to CO_2 (K ppmv^{-1}), β_{AB} and β_{AO} are the land and ocean carbon cycle sensitivity to atmospheric CO_2 (GtC ppmv–1), γ_{AB} and γ_{AO} are the land and ocean carbon cycle sensitivity to climate change (GtC K^{-1}), g is the gain of the feedback, namely the relative increase of atmospheric CO_2 due to the feedback, and f is the net feedback factor defined as 1/(1 _ g). For the calculation of γ_{AB} and γ_{AO}, we isolated the direct climate impact on the fluxes from the indirect climate effect through increased atmospheric CO_2 [9].

Another result of the integrated model experiment is depicted in Fig. 3, which shows distribution of anthropogenic CO_2 accumulated in the ocean until 1994 from the coupled run and observations [16]. The simulated anthropogenic CO_2 is estimated as the difference between total inorganic carbon (TIC) and another tracer calculated in the same way as TIC but with the fixed atmospheric CO_2 concentration of 285 ppmv. It is seen in both the simulation and the observations that the northern North Atlantic and the Southern Ocean, where deep waters are being formed, are capable of carrying much CO_2. It can be said that the simulation and the observations show overall agreement on the global and a basin scale. In particular, since it has been pointed out that the greatest uncertainty regarding oceanic uptake of anthropogenic CO_2 is found in the Southern Ocean [14, 17], it is encouraging that our model shows a reasonable match for Southern Ocean storage in both the magnitude and the latitudinal extent. The cumulative anthropogenic CO_2 until 1994 is 98 PgC in the model, and close to the lower limit of the observation-based estimate of 118 ± 19 PgC [16], which may include a bias toward a larger value by 7% due to the assumption of constant disequilibria between atmospheric and oceanic CO_2 partial pressures [18].

2.3 Development of a new dynamic vegetation model

The terrestrial carbon cycle model in our integrated model, Sim-CYCLE does not represent change of vegetation type caused by environmental conditions; only the growth rate NPP of the prescribed vegetation type changes in response to changing climate. In order to extend the model to allow alteration of vegetation types, processes that cause such change, namely establishment, competition, mortality, and so on must be introduced. For representing such dynamic changing of vegetation we decided to develop an individual-based, dynamic global vegetation model (DGVM) named Spatially-Explicit Individual-Base DGVM (SEIB-DGVM). Namely, we consider several sample forests or grasslands of a small area (30m × 30m) placed at each grid box and calculate growth and decay of individual trees in each small area by explicit calculation of tree height crown diameter, crown depth and so forth by considering light conditions of each tree surrounded by other trees. By doing so we expect that the speed of alteration of one vegetation type to another will be represented reasonably without introducing any additional parameterizations. Such individual-based model for a small plot has already been developed (e.g., SORTIE [19, 20]) and verified in many biomes.

In representing vegetation types we adopt plant functional types (PFTs) used in LPJ-DGVM [21] and the parameter needed for some important processes, e.g., establishment, mortality due to heat stress and so on are also obtained from LPJ-DGVM. At present, experiments for single plot areas inhabited by multiple PFTs have been performed and the results are being examined. An example of preliminary calculations is shown in Fig. 4. Upgrading the model to a continental or the global scale is underway and the results will be reported elsewhere.

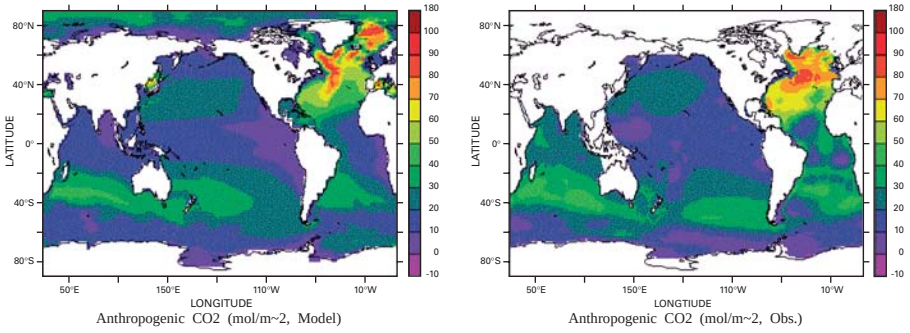

Fig. 3 Distribution of anthropogenic CO_2 stored in the ocean. (left) Model result and (right) observations [16]. Units are molC/m^2.

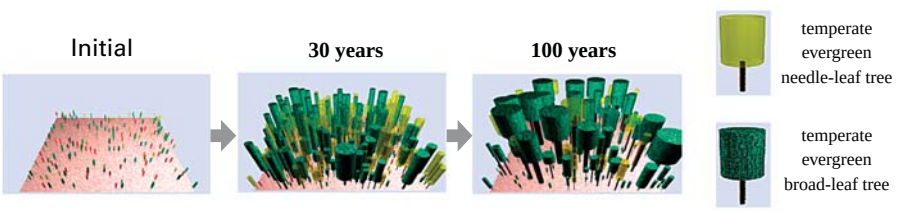

Fig. 4 An example of the results of landscape simulations (valid for Kumamoto).

3. Atmospheric chemistry-climate coupling

As climate change feeds back to the concentration of CO_2, it also affects the concentration of other atmospheric constituents such as ozone (O_3), methane (CH_4) and aerosols which are active in thermal radiation or have effects to modify clouds, and hence have feedbacks to climate change. Therefore to predict both atmospheric composition change and climate change correctly, coupling of those two processes is needed.

3.1 Tropospheric chemistry and aerosols in the climate and global environment systems

The chemical composition of the atmosphere has been changed largely by increase in anthropogenic emissions associated with industry, car traffic, and land use. In addition to well-mixed gases like CO_2 and CH_4, reactive species such as ozone (O_3) and its precursors (carbon monoxide CO, nitrogen oxides NO_x, nonmethane hydrocarbons NMHCs etc.) and aerosols have been increased globally over the past century [22, 23] as anthropogenic emissions have risen dramatically. In particular, severalfold increase of ozone has been observed in the northern midlatitudes since preindustrial times. While ozone in the stratosphere (ozone layer) has a beneficial role to shield us from sun (ultraviolet) light, tropospheric ozone displays a destructive side. Since ozone reacts strongly with other molecules, it can severely damage the human health and plants including some important agricultural crops [24, 25], and is a key pollutant in smog hanging over many cities around the world. In addition, tropospheric ozone is a significant greenhouse gas that absorbs both longwave (terrestrial) and shortwave (solar) radiation [26]. The effect of tropospheric ozone increase on climate since preindustrial times has typically been estimated to be a radiative forcing between 0.3 and 0.5 W m^{-2} [e.g., 27, 28, 29], comparable with the estimated methane forcing. It should be noted that the radiative forcing from tropospheric ozone is distributed inhomogeneously like aerosols forcing, being generally larger in polluted areas particularly in the Northern Hemisphere, because of its short lifetime. Ozone has also a critical importance for tropospheric photochemistry to activate chemical reactions and control the lifetime of other chemical species (oxidizing capacity) through formation of hydroxyl radical (OH). Tropospheric ozone chemistry definitely controls the lifetimes and hence the levels of CH_4 and HFCs. This 'indirect' effect of tropospheric chemistry has been shown to make a significant contribution to the total radiative forcing [30, 31, 32]. Also, ozone chemistry plays an important role in the formation process of sulfate ($SO4^{-}$) aerosol, a major cause of acid rain, which has direct (sunlight scattering) and indirect (cloud condensation nuclei, CCN) climate effects. Tropospheric ozone chemistry, therefore, acts as an important interface for both the climate system and atmospheric environment. Furthermore, it should be noted that ozone chemistry in the atmosphere, being dependent much on meteorological variables such as water vapor, temperature, and large-scale circulation, interacts with climate change.

3.2 Atmospheric chemistry and aerosols modeling in the integrated earth system model

On the backgrounds as described above, we have been developing an atmospheric chemistry-aerosols coupled climate model in the framework of the Kousei-2 Earth system modeling project on the ES. Although our chemistry modeling is much focused on tropospheric ozone chemistry at this stage, our overall modeling plan involves simulation of stratospheric ozone with halogen chemistry and polar stratospheric clouds (PSCs) chemistry as well. Fig. 5 gives an overview of our chemistry-aerosols modeling. For simulations of tropospheric chemistry and aerosols, we use the chemistry coupled climate model CHASER [33] in cooperation with aerosol model SPRINTARS [34], both of which are based on the CCSR/NIES climate model. Our chemistry-aerosols model considers anthropogenic and natural emissions of precursors like NO_x, CO, NMHCS, and SO_2, as well as direct emissions of carbonaceous, soil-dust, and sea-salt aerosols. CHASER simulates subsequent photochemistry in gas/liquid phase reactions, and heterogeneous reactions on aerosols surface with considering dry/wet deposition as well. It also includes a detailed scheme for sulfate aerosol simulation, calculating liquid-phase oxidation of SO_2 by H_2O_2 and O_3 to form sulfate in clouds with neutralization of cloud acidity (pH) by ammonium (NH_4^+) and mineral cations such as Ca^{2+} and Mg^{2+} originating from soil-dust. Distributions of greenhouse gases as O_3, CH_4, and N_2O, and aerosols computed in the chemistry-aerosols component are reflected on-line on the GCM radiation calculation. The aerosols indirect effects on clouds are also taken into account in the framework of SPRINTARS. The chemistry-aerosols model based on CHASER and SPRINTARS is being implemented in the Kyouse-2 Earth system model (KISSME) on ES, and this would enable us to perform a fully coupled simulation of climate, atmospheric chemistry-aerosols, ocean, and land surface.

3.3 Preliminary studies on chemistry-climate interaction with the ES

Though our present modeling works have been basically focused on development of our atmospheric chemistry-aerosols model, we have conducted several off-line calculations to investigate future/past climate change impacts

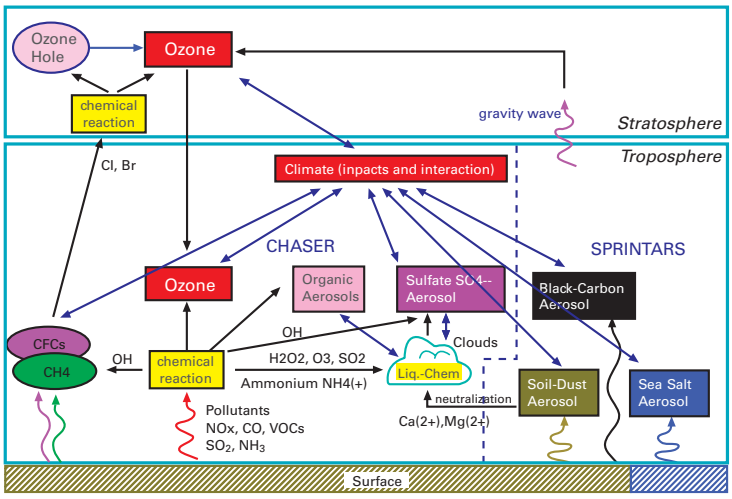

Fig. 5 Schematic illustration of atmospheric chemistry-aerosols coupled submodeling in the framework of the Kyousei-2 Earth system model integration. The present model, including detailed simulation of photochemistry and aerosols in the troposphere, considers effects of changes in thermally active species such as O_3 and CH_4, and aerosols on radiation and clouds.

on tropospheric ozone chemistry (including CH_4) and aerosols. For future projection, we have simulated global distributions and budgets of O_3, CH_4, and sulfate aerosol for the 21st century following the IPCC/SRES scenarios [35]. The simulation employs the chemistry climate model CHASER driven on-line by the CCSR/NIES atmospheric GCM [33] (described above). The model uses the horizontal resolution of T42 (~2.8° x 2.8°) with 32 layers in the vertical through the simulations. To assess emission change impacts and climate change impacts on tropospheric chemistry independently, we conduct two experiments: (Exp1) a control experiment only with changes in ozone precursor (NO_x, CO, etc.) emissions and (Exp2) an experiment with climate change as well as emission changes. In Exp1 GCM simulates present-day climate using the present greenhouse gases levels and sea surface temperatures (SSTs), but in Exp2 it simulates climate change using greenhouse gases evolving with the IPCC SRES scenarios. In Exp2, other forcing factors such as SSTs and sea ice distributions are also prescribed by the transient simulations with the CCSR/NIES coupled atmosphere-ocean GCM [36, 37] (with no flux adjustment) for the SRES scenarios. In both experiments, future anthropogenic emissions of O_3 precursors and CH_4 are specified by the SRES scenarios. Neither Exp1 nor Exp2 considers future changes in stratospheric ozone abundances; both use the same stratospheric ozone distributions as prescribed in a present-day simulation.

Fig. 6 shows the temporal evolution of global mean CH_4 concentration projected for 2000-2100 with three different SRES scenarios (A2, A1, and B1). The global CH_4 trend calculated in Exp1, only with emission changes, basically reflects CH_4 emissions specified with each scenario. The emission-induced CH_4 change, however, appears to be reduced significantly by climate change in Exp2 for each scenario. This negative feedback from climate change to CH_4 is caused by increases in water vapor and temperatures associated with tropospheric warming in Exp2 which enhance the CH_4 loss reaction with OH radical (CH_4 + OH). In particular, increases in water vapor enhance the OH level via photochemical reactions, resulting in enhanced CH_4 loss in the troposphere. It should be noted that although magnitude of the projected climate change is much dependent on scenario, our simulation shows a CH_4 reduction by ~20% due to climate change in 2100 for all three scenarios.

In Exp1 only with changes in emissions of O_3 precursors (NO_x, CO, etc.), significant increases in surface O_3 are calculated in eastern Asia in response to enhanced chemical production of ozone with the prescribed emission increases (e.g., Fig. 7 for the A2 scenario). Our simulations also show that enhanced ozone production in the upper troposphere over eastern Asia has a huge impact on future global distributions of ozone owing to rapid intercontinental transport out of the region.

However, our study suggests that these changes in tropospheric ozone with emission changes can be modulated by future climate change (warming). In Exp2 with climate change, lower tropospheric ozone levels are reduced in comparison with Exp1 due to increased chemical loss of ozone associated with the water vapor increases. Upper tropospheric ozone in the high latitudes also decreases

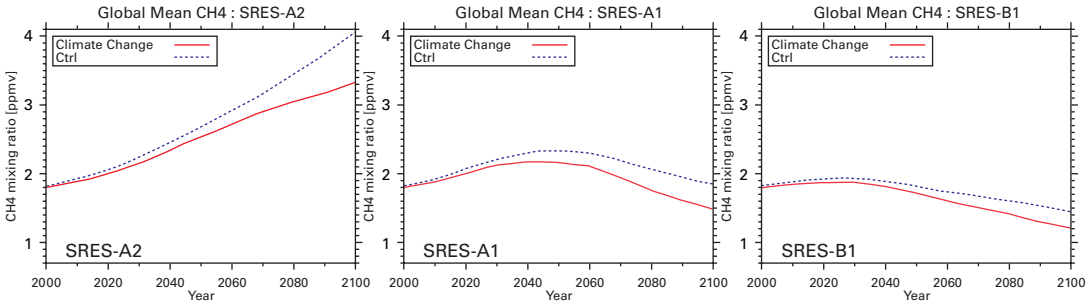

Fig. 6 Temporal evolution of global mean methane concentrations projected for SRES (left) A2 which is a high case, (middle) A2 which is an intermediate case, (right) B1 which is a low case from 2000 to 2100. Solid lines show results from the simulations with climate change as well as emission changes (Exp2), with dashed lines for the control simulations (Exp1) with emission changes only (using present climate).

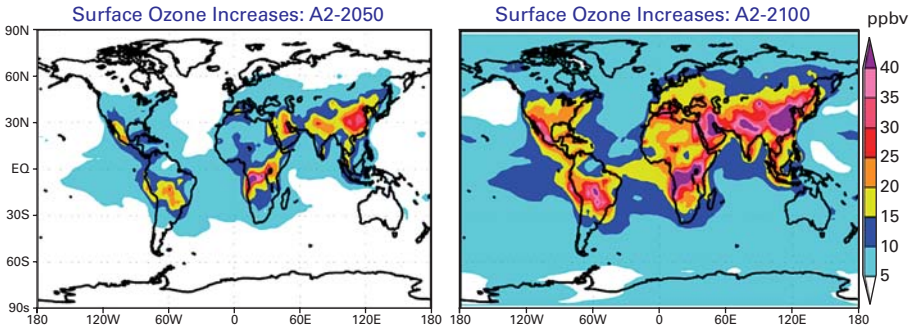

Fig. 7 Surface ozone increases (ppbv) predicted for (left) 2050 and (right) 2100 with the IPCC SRES-A2 emission scenario. Surface ozone levels in eastern Asia are simulated to increase by ~50% in 2050 and by ~100% in 2100 relative to the present-day.

reflecting the rises in the tropopause height induced by climate change (not shown). On the other hand, the model shows increases in upper tropospheric ozone in the low-mid latitudes due to climate change. These ozone increases are attributed to the enhanced ozone input from the stratosphere. As Fig. 8 shows, the experiment with climate change (Exp2) shows increases in O_3 stratosphere/troposphere exchange, STE, (net O_3 influx to the troposphere) calculating an STE of as much as 1100 TgO_3/yr in 2100 (+83% relative to 1990). This suggests that future climate change induces increases in downward cross-tropopause O_3 flux which exceed enhancements in upward tropospheric O_3 transport caused by increased O_3 in the troposphere due to emission increases. The key factor controlling the STE O_3 increases in Exp2 is the change in the residual (meridional) circulation in the model. We found increases in the Brewer-Dobson circulation and the Hadley circulation due to climate change, which cause enhanced ascent in the tropics and descent in the subtropical lower stratosphere. In response to the enhanced stratospheric O_3 transport, the emission-induced O_3 increases in the upper troposphere as calculated in the control experiment (Exp1) are further enhanced in the climate change experiment (Exp2). The net chemical O_3 production within the troposphere estimated for 2100 is 740 TgO_3/yr in Exp1 but - 4.7 TgO_3/yr in Exp2 reflecting enhanced O_3 destruction due to the water vapor increases especially in the lower troposphere and increase of O_3 itself caused by the vigorous STE in Exp2 as described above.

Fig. 9 shows the evolution of sulfate burden calculated for 1990 to 2100 in Exp1 and Exp2. In response to SO_2 emission increases, sulfate burden increases to 0.9-1 TgS/yr in 2030-2050 for both Exp1 and Exp2. A remarkable result is that sulfate burdens after 2070 are still larger than in 1990 or 2000, though SO_2 emission levels after 2070 are assumed to become lower than those in 1990-2000. The larger sulfate burdens after around 2080 in Exp1 are attributed to enhanced liquid-phase sulfate formation with H_2O_2 particularly in the low latitudes where significant H_2O_2 increases are predicted. In the case of Exp2, the changes in clouds and precipitation associated with climate change in the model also contribute to the additional increases in sulfate burden after around 2030.

Our preliminary results for future CH_4, O_3, and sulfate aerosol as described above imply that for prediction of future climate and atmospheric environment, it is necessary to take into account the feedbacks from climate change as well as emission changes.

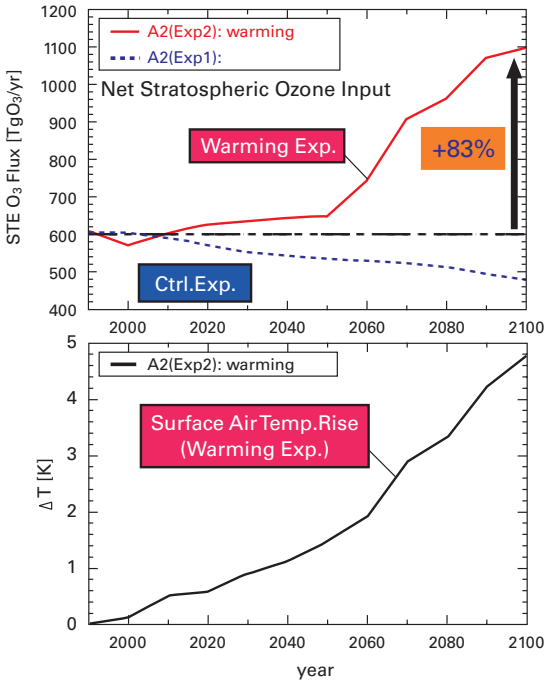

Fig. 8 (Top): temporal evolution of net stratospheric ozone influx to the troposphere for 1990-2100 calculated in the climate change (warming) and control experiment. (Bottom): global and annual mean surface air temperature change relative to 1990 in the warming experiment. The decreases in net stratospheric ozone input in the control experiment are due to increases in tropospheric ozone with the emission increases.

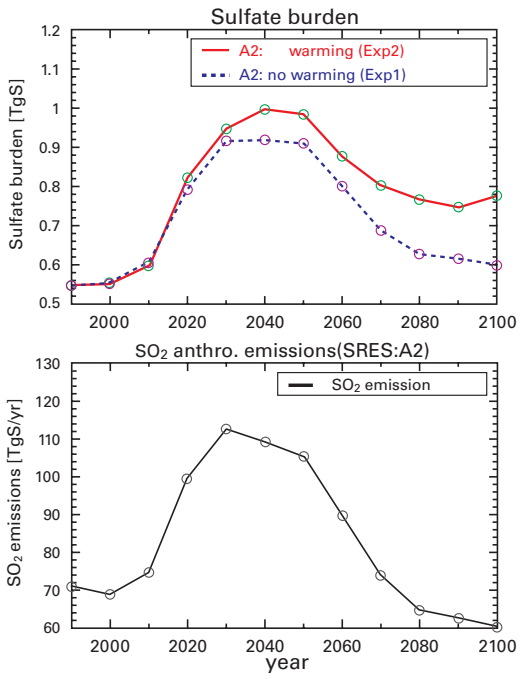

Fig. 9 (Top) global sulfate burdens for 1990-2000 simulated in Exp1 and Exp2 with the SRES A2 scenario. (Bottom) global anthropogenic SO_2 emissions prescribed by the A2 scenario.

4. Improvement of the physical climate system model

4.1 Improvement of the AGCM

In the integrated earth system modeling we plan to include physical and chemical processes in the middle atmosphere more thoroughly, i.e., the stratosphere and mesosphere, because climate and other environmental conditions in the troposphere are coupled with the middle atmosphere in many ways [38]. A specific example is the change of the tropospheric ozone due to change of stratosphere/troposphere exchange as discussed in the previous section. In considering coupling between the troposphere and the middle atmosphere, the first is dynamical coupling through vertically propagating atmospheric waves with various horizontal scales. The waves 1) transport momentum and energy upward from the troposphere to the middle atmosphere, 2) interact with mean flows and induce meridional circulations which cause dynamical heating/cooling as well as transport and mixing of chemical species, and 3) induce local perturbations in temperature, resulting in variations in chemical species.

Dynamical exchange of chemical species across the tropopause is mainly caused by the meridional circulation, i.e., the Brewer-Dobson circulation, and eddy transport along isentropic surfaces, along with deep convection in the tropics [38, 39]. Such stratosphere-troposphere exchange is crucial for climate change, because it modifies concentrations of radiatively active gases, e.g., ozone, CH_4 and water vapor, in both the troposphere and the stratosphere.

Another important issue is springtime polar ozone depletion known as the ozone hole. It enhances interannual variability of springtime polar night jet, and probably affects the tropospheric general circulation [40]. Development of the Antarctic ozone hole depends not only on concentrations of anthropogenic halocarbons, but also on dynamical stability of the polar vortex and temperatures in the polar lower stratosphere.

In order to model abovementioned issues properly, some substantial improvements have been made for the AGCM. They are summarized as follows; 1) the upper limit of the model is extended to about 0.01 hPa, 2) a vertical resolution in the stratosphere is increased (~650 m) to realize the equatorial quasi-biennial oscillation (QBO) and stratopause semi-annual oscillation (SSAO) (cf. [41, 42, 43]), 3) the original σ-vertical coordinate system is replaced by a σ-p hybrid vertical coordinate system to avoid artificial horizontal advection in downstream of

mountains [44], 4) an updated version of radiation scheme is employed to decrease cold biases near the tropical tropopause and the summertime lower stratosphere, and 5) a non-orographic gravity wave drag (GWD) parameterization of Hines [45, 47] is employed to obtain a realistic seasonal march of the polar vortex (by eliminating the cold pole bias problem), as well as the equatorial QBO and SSAO. The GWD parameterization is necessary because the standard horizontal resolution of the AGCM is T42, which is not fine enough to explicitly resolve gravity waves effective to large scale stratospheric circulation.

4.2 High-resolution AGCM simulations

The Hines scheme requires information on global distribution and characteristics of gravity waves, which are difficult to evaluate from observations. In order to obtain information on global morphology of gravity waves and their propagation direction and momentum fluxes, we performed several high-resolution AGCM simulations (e.g., [43, 47, 48]). Here, results of two AGCM simulations with different horizontal resolutions are compared. This comparison is analogous to what has been conducted for the GFDL SKYHI GCM simulations [49].

The horizontal resolutions are T106 and T213. The minimal resolvable horizontal wavelengths are about 380 km and 190 km, respectively. Other experimental settings are almost the same for each other. The AGCM has 250 layers from the surface to 0.01 hPa. A vertical resolution is 300 m throughout the middle atmosphere. The AGCM includes realistic topography and a full set of physical parameterizations [50]. Any GWD parameterizations are excluded for these simulations in order to focus on explicitly resolved gravity waves. Results are shown as monthly averages of June in a typical year of each simulation.

Fig. 10 shows contour plots of the zonal mean zonal winds for the T213 and T106 simulations (referred to as T213 and T106 hereafter). Colors show the zonal mean vertical fluxes of zonal momentum ($\overline{u'\omega'}$) due to $k > 5$ components, where k denotes the zonal wavenumber. In the tropics, several vertical reversals of the zonal wind are seen. They show structures of the QBO, SSAO, and intraseasonal oscillation in the mesosphere (cf. [43]).

The maximum wind speed of the polar night jet is ~100 ms^{-1} for T213, while ~130 ms^{-1} for T106. Similarly, the maximum wind speed of the summertime easterly jet in the mesosphere is weaker in T213 (~ 50 ms^{-1}) than in T106 (~ 60 ms^{-1}). These wind maxima are located at lower altitudes in T213. Moreover, the core of the polar night jet is located at a lower latitude in T213, corresponding to warmer temperature in high latitudes in the whole stratosphere (not shown). The weaker zonal winds in T213 mesosphere are more realistic than in T106 (cf. CIRA86 [51]). This fact suggests that zonal flow decelerations due to gravity waves are larger and more realistic in T213 than in T106.

Signs of the zonal momentum fluxes are negative in the southern hemisphere middle atmosphere, and positive in the northern hemisphere above the zero wind line. This indicates dominance of upward transport of easterly (westerly) momentum relative to the wintertime westerly (summertime easterly). The zonal momentum is generally carried by vertically propagating gravity waves generated in the troposphere. Decreases of the momentum fluxes in the mesosphere are due to wave breaking and saturation processes. Resultant vertical divergence of the zonal momentum flux leads to decelerations of the zonal winds. Hence, the weaker zonal winds in the T213 mesosphere are attributable to larger vertical divergence of the zonal momentum fluxes as seen in Fig. 10.

Fig. 11 shows differences in the zonal mean zonal wind and momentum fluxes between T213 and T106. Magnitude of the zonal momentum fluxes is much larger in T213 than in T106 in both the summer and winter hemispheres, especially for the mid- and high latitudes

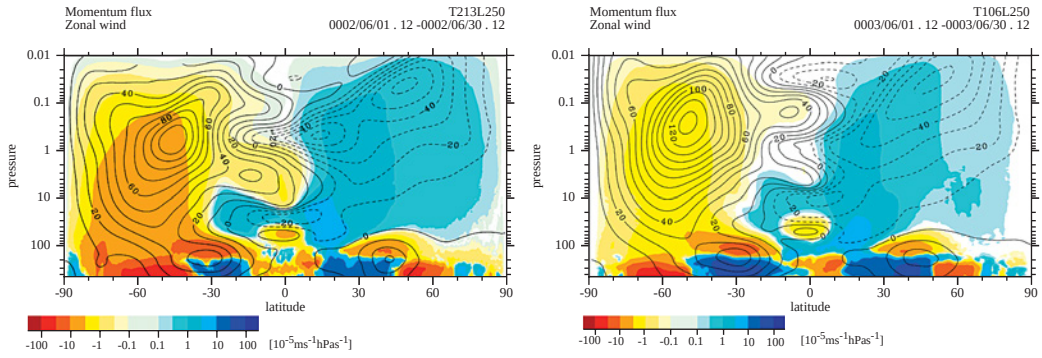

Fig. 10 Contour: Zonal mean zonal wind in ms^{-1}. Color: Zonal mean vertical flux of zonal momentum ($\overline{u'\omega'}$) due to k > 5 components in 10^{-1} $ms^{-1}hPas^{-1}$. Color scale is set logarithmically. Horizontal resolution is (left) T213 and (right) T106.

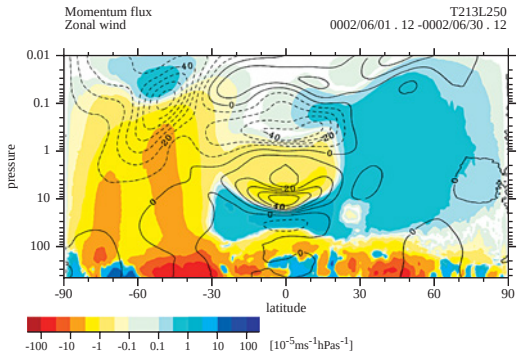

Fig. 11 As in Fig. 10, but for differences between T213 and T106.

where T213 values are about twice as large as those for T106 (see also Fig 10). In the southern hemisphere, two bands of large negative momentum fluxes extend vertically from the troposphere to the upper stratosphere. The high latitude one is largely attributable to enhanced orographic gravity waves over Antarctica, because of finer topography in T213 [52]. The mid-latitude one is probably brought about by enhanced generation of small-scale gravity waves by cumulus convection involved in extratropical cyclones as well as orographic generation over the Andes. A positive difference in the upper mesosphere means occurrence of wave breaking in lower altitudes. That may result from larger gravity wave amplitudes. In the northern hemisphere where orographic gravity waves encounter their critical levels in the troposphere and lower stratosphere, increases in positive momentum fluxes are largely attributable to increases in small-scale gravity waves generated by "mesoscale" convective systems generated in these AGCMs. Some of them are involved in extratropical cyclones, while others are well-developed convective cloud clusters over continents [47].

The increase in horizontal resolution of the AGCM leads to the increase in momentum fluxes due to small-scale gravity waves, resulting in more realistic general circulation in the middle atmosphere. This result is qualitatively similar to those obtained by the SKYHI simulations [49]. We employed higher vertical resolution (L250) than for SKYHI and obtained the polar night jet maximum at lower latitude (~45°S) compared to their results. We also obtained the second peak of westerly in high latitude mesosphere. These characteristics are quite realistic. However, the maximum wind speed of the polar night jet is slightly stronger than observed (CIRA86 [51]), showing a necessity of higher horizontal resolutions. The finer horizontal resolution (T213) results are being analyzed to estimate the source information of gravity waves required by the GWD parameterization [48]. This effort will provide realistic simulations for the atmospheric chemistry and climate.

5. Summary and outlook

Kyousei-2 is a project to develop a model where biogeochemistry and physical climate system interact with each other. The development is conducted by coupling existing biogeochemical component models with an atmosphere-ocean coupled climate model. As of August 2005, the current version of the integrated model includes carbon cycle for both land and ocean, and tropospheric chemistry. It is planned to extend the model top, which is currently ~ 30 km, to the upper stratosphere with a sophisticated parameterization of gravity wave drag. An individual-based dynamic global vegetation model is being developed and to be incorporated in the integrated model by the end of the project in FY 2006. Results from a preliminary experiment for climate – carbon cycle feedbacks show significant differences from those of two preceding studies necessitating a cooperative investigation to identify their cause (s) under the framework of, e.g., C4MIP. Experiments with the atmospheric chemistry component model CHASER show that there are significant differences in future atmospheric composition projected by the model depending on whether one considers interactions between climate change and chemical reactions in the atmosphere. While attempting to improve gravity wave drag parameterization for the stratosphere, it has been revealed that gravity wave drag directly derived from explicitly resolved gravity waves shows significant dependence on the resolution.

As a whole, the project exhibits a steady progress. It is expected that the integrated model, when completed, will profit the entire community for climate research by enabling direct researches on interactions among sub-systems that have formerly been studied in separate disciplines.

Acknowledgments

The authors would like to thank the members of the Kyousei-1 project (P. I.: Prof. A. Sumi), who kindly provided their climate model for further extension by the Kyousei-2 project. Drs. S. Emori,

K. Ichii, and A. Ito helped the incorporation of SimCYCLE into our atmospheric general circulation model. Ms. M. Aita installed carbon cycle component in our ocean general circulation model.

(This article is reviewed by Dr. Julia Slingo.)

References

[1] P. Cox, R. Betts, C. Jones, S. Spall and I. Totterdell, Acceleration of global warming due to carbon-cycle feed-

backs in a coupled climate model, *Nature*, vol.**408**, pp.184–187, 2000.

[2] P. Friedlingstein, L. Bopp, P. Ciais, J.-L. Dufresne, L. Fairhead, H. LeTreut, P. Monfray and J. Orr, Positive feedback between future climate change and the carbon cycle, *Geophysical Research Letters*, vol.**28**, pp.1543–1546, 2001.

[3] K. Sudo, M. Takahashi, and H. Akimoto, Future changes in stratosphere-troposphere exchange and their impacts on fugure tropospheric simulations, *Geophysical Research Letters*, vol.**30**, 24, 2256, doi:10.1029/2003GL018526, 2003.

[4] A. Ito and T. Oikawa, A simulation model of the carbon cycle in land ecosystems Sim-CYCLE: A description based on dry-matter production theory and plot-scale validation, *Ecological Modelling*, vol.**151**, pp.147–179, 2002.

[5] A. Ito, Climate-related uncertainties in projections of the 21st century terrestrial carbon budget: Off-line model experiments using IPCC greenhouse gas scenarios and AOGCM climate projections, *Climate Dynamics*, 2005 (in press).

[6] A. Ito, Regional variability in the terrestrial carbon-cycle response to global warming in the 21st century: simulation analysis with AOGCM-based climate projections, *Journal of the Meteorological Society of Japan*, 2005 (in press).

[7] M. Aita, N., Y. Yamanaka and M. J. Kishi, Effect of ontogenetic vertical migration of zooplankton on annual primary production — Using NEMURO embedded in general circulation model —, *Fish. Oceanogr*, vol.**12**, pp.284–290, 2003.

[8] A. Oschlies, and V. Garçon, An eddy-permitting coupled physical-biological model of the North Atlantic 1. Sensitivity to advection numerics and mixed layer physics, *Global Biogeochemical Cycles*, vol.**13**, pp.135–160, 1999.

[9] A. Oschlies, Model-derived estimates of new production: New results point towards lower values, *Deep-Sea Research II*, vol.**48**, pp.2173–2197, 2001.

[10] H. Hasumi, and S. Emori, K-1 Coupled GCM (MIROC) Description, *K-1 Technical Report No.1*, Center for Climate System Research (Univ. of Tokyo), National Institute for Environmental Studies, and Frontier Research Center for Global Change, 2004.

[11] I. C. Prentice, M. T. Sykes, M. Lautenschlager, S. P. Harrison, O. Denissenko and P. J. Bartlein, Modelling vegetaion patterns and terrestrial carbon sorage at the last glacial maximum, *Global Ecology and Biogeography Letters*, vol.**3**, pp.67–76, 1993.

[12] L. M. François, C. Delire, P. Warnant and G. Munhoven, Modelling the glacial-interglacial changes in the continental biosphere, *Global and Planetary Change*, vol.**16–17**, pp.37–52, 1998.

[13] J. M. Adams and H. Faure, A new estimate of changing carbon storage on land since the last glacial maximum, based on global land ecosystem reconstruction, *Global and Planetary Change*, vol.**16–17**, pp.3–24, 1998.

[14] P. Friedlingstein, J.-L. Dufresne, P. M. Cox and P. Rayner, How positive is the feedback between climate change and the carbon cycle, *Tellus*, vol.**55B**, pp.692–700, 2003.

[15] J.-L. Dufresne, P. Friedlingstein, M. Berhelot, L. Bopp, P. Ciais, L. Fairhead, H. LeTreut and P. Monfray, On the Magnitude of Positive Feedback between Future Climate Change and the Carbon Cycle, Geophysical Research Letters, vol.**29**, doi:10.1029/2001GL013777, 2002.

[16] C. L. Sabine, R. A. Feely, N. Gruber, R. M. Key, K. Lee, J. L. Bullister, R. Wanninkhof, C. S. Wong, D. W. R. Wallace, B. Tilbrook, F. J. Millero, T.-H. Peng, A. Kozyr, T. Ono, and A. F. Rios, The Oceanic Sink for Anthropogenic CO_2, *Science*, vol.**305**, pp.367–371, 2004.

[17] J. C. Orr, E. Maier-Reimer, U. Mikolajewicz, P. Monfray, J. L. Sarmiento, J. R. Toggweiler, N. K. Taylor, J. Palmer, N. Gruber, C. L. Sabine, C. LeQuèrè, R. M. Key and J. Boutin, Estimates of anthropogenic carbon uptake from four three-dimensional global ocean models, *Global Biogeochemical Cycles*, vol.**15**, pp.43–60, 2001.

[18] K. Matsumoto and N. Gruber, How accurate is the estimation of anthropogenic carbon in the ocean? An evaluation of the ΔC^* method, Global Biogeochemical Cycles, in press, 2005.

[19] S. W. Pacala, C. D. Canham, and J. A. J. Silander., Forest models defined by field measurements: I. The design of a northeastern forest simulator, *Can. J. For. Res*., vol.**23**, pp.1980–1988, 1993.

[20] S. W. Pacala, C. D. Canham, and A. J. Silander, R. K. Kobe, and E. Ribbens. Forest models defined by field measurements: Estimation, error analysis and dynamics. Ecol, *Monogr*., vol.**66**, pp.1–43, 1996.

[21] S. Sitch, B. Smith, I. C. Prentice, A. Arneth, A. Bondeau, W. Cramer, J. O. Kaplan, S. Levis, W. Lucht, M. T. Sykes, K. Thonicke, and S. Venevsky, Evaluation of ecosystem dynamics, plant geography and terrestrial carbon cycling in the LPJ dynamic global vegetation model, *Global Change Biology*, vol.**9**, pp.161–185, 2003.

[22] WMO, Report of the International Ozone Trends Panel: 1988, Global Ozone Research and Monitoring Project: Report No.18, Geneva, 1990.

[23] P. J. Crutzen and P. H. Zimmermann, The changing photochemistry of the troposphere, *Tellus*, vol.**43**, pp.136–151, 1991.

[24] World Health Organization (WHO), Update and revision of the WHO air quality guidelines for Europe. Classical air pollutants: ozone and other photochemical oxidants, European centre for environment and health, Bilthoven, the Netherlands, 1996.

[25] World Health Organization (WHO), Update and revision

of the WHO air quality guidelines for Europe. Ecotoxic effects, ozone effects on vegetation, European centre for environment and health, Bilthoven, the Netherlands, 1996.

[26] W. Wang, J.P. Pinto, and Y.L. Yung, Greenhouse effects due to man-made perturbations of trace gases, *J. Atmos. Sci*., vol.**37**, pp.333–338, 1980.

[27] P. M. Forster, C. E. Johnson, K. S. Law, J. A. Pyle, and K. P. Shine, Further estimates of radiative forcing due to tropospheric ozone changes, *Geophys. Res. Lett*., vol.**23**, pp.3321–3324, 1996.

[28] T. K. Berntsen, I. S. A. Isaksen, G. Myhre, J. S. Fuglestvedt, F. Stordal, T. Alsvik, Larsen, R. S. Freckleton, and K. P. Shine, Effects of anthropogenic emissions on tropospheric ozone and its radiative forcing, *J. Geophys. Res*., vol.**102**, pp.28,101–28,126, 1997.

[29] L. J. Mickley, P. P. Murti, D. J. Jacob, J. A. Logan, D. M. Koch, and D. Rind, Radiative forcing from tropospheric ozone calculated with a unified chemistry-climate model, *J. Geophys. Res*., vol.**104**, pp.30,153–30,172, 1999.

[30] D. A. Hauglustaine, C. Granier, G. P. Brasseur, and G. Megie, The importance of atmospheric chemistry in the calculation of radiative forcing on the climate system, *J. Geophys. Res*., vol.**99**, pp.1173–1186, 1994.

[31] C. E. Johnson and R. G. Derwent, Relative radiative forcing consequences of global emissions of hydrocarbons, carbon monoxide and NOx from human activities estimated with a zonally averaged two-dimensional model, *Climate Change*, vol.**34**, pp.439–462, 1996.

[32] O. Wild, M.J. Prather, and H. Akimoto, Indirect long-term global radiative cooling from NOx emissions, *Geophys. Res. Lett*., vol.**28**, pp.1719–1722, 2001.

[33] K. Sudo, M. Takahashi, J. Kurokawa, and H. Akimoto, CHASER: A global chemical model of the troposphere 1. Model description, *J. Geophys. Res*., vol.**107**, doi:10.1029/2001JD001113, 2002.

[34] T. Takemura, H. Okamoto, Y. Maruyama, A. Numaguti, A. Higurashi, and T. Nakajima, Global three-dimensional simulation of aerosol optical thickness distribution of various origins, *J. Geophys. Res*., vol.**105**, pp.17,853–17,873, 2000.

[35] K. Sudo., M. Takahashi, and H. Akimoto, Future changes in stratosphere-troposphere exchange and their impacts on future tropospheric ozone simulations Geophys. Res. Letters., vol.**30**, 2256, doi:10.1029/2003GL018526, 2003.

[36] S. Emori, T. Nozawa, A. Abe-Ouchi, A. Numaguti, M. Kimoto, and T. Nakajima, Coupled ocean-atmosphere model experiments of future climate change with an explicit representation of sulfate aerosol scattering, *J. Meteor. Soc. Japan*, vol.**77**, pp.1299–1307, 1999.

[37] T. Nozawa, S. Emori, A. Numaguti, Y. Tsushima, T. Takemura, T. Nakajima, A. Abe-Ouchi, and M. Kimoto, Projections of future climate change in the 21st century simulated by the CCSR/NIES CGCM under the IPCC SRES scenarios, in Present and Future of Modeling Global Environmental Change toward Integrated Modeling, ed. T. Matsuno and H. Kida, Terra Scientific Publishing, pp.15–28, 2001.

[38] T. G. Shepherd, Issues in stratosphere-troposphere coupling, *J. Meteor. Soc. Japan*, vol.**80**, no.4B, pp.769–792, 2002.

[39] J. R. Holton, P. H. Haynes, M. E. McIntyre, A. R. Douglass, R. B. Rood, and L. Pfister, Stratosphere-troposphere exchange, *Rev. Geophys*, vol.**33**, no.4, pp.403–409, 1995.

[40] S. Watanabe, T. Hirooka, and S. Miyahara, Interannual variations of the general circulation and polar stratospheric ozone losses in a general circulation model, *J. Meteor. Soc. Japan*, vol.**80**, no.4B, pp.877–895, 2002.

[41] M. Takahashi, Simulation of the stratospheric quasi-biennial oscillation using a general circulation model, *Geophys. Res. Lett*., vol.**23**, no.6, pp.661–664, 1996.

[42] M. Takahashi, Simulation of the quasi-biennial oscillation using a general circulation model, *Geophys. Res. Lett*., vol.**26**, no.9, pp.1307–1310, 1999.

[43] S. Watanabe, and M. Takahashi, Kelvin waves and ozone Kelvin waves in the QBO and SAO; a simulation by a high-resolution chemistry-coupled GCM, *J. Geophys. Res*., vol.**110**, no. 18, D18303, doi:10.1029/2004JD005424, 2005.

[44] H. Miura, Vertical differencing of the primitive equations in a Sigma-p hybrid coordinate (for spectral AGCM), CCSR *internal report*, pp.1–19, University of Tokyo, 2002.

[45] C. O. Hines, Doppler-spread parameterization of gravity–wave momentum deposition in the middle atmosphere. Part 1: Basic formulation, *J. Atmos. Solar Terr. Phys*., vol.**59**, no.4, pp.371–386, 1997.

[46] C. O. Hines, Doppler-spread parameterization of gravity–wave momentum deposition in the middle atmosphere. Part 2: Broad and quasi monochromatic spectra, and implementation, *J. Atmos. Solar Terr. Phys*., vol.**59**, no.4, pp.387–400, 1997.

[47] S. Watanabe, An explicit simulation of gravity waves using a T213L250 middle atmosphere GCM Part I: GCM results, in preparation, 2005.

[48] S. Watanabe and T. Nagashima, An explicit simulation of gravity waves using a T213L250 middle atmosphere GCM Part II: implications for gravity wave drag parameterizations, in preparation, 2005.

[49] K. Hamilton, R. J. Wilson, and R. S. Hemler, Middle atmosphere simulated with high vertical and horizontal resolution versions of a GCM: Improvements in the cold pole bias and generation of a QBO-like oscillation in the tropics, *J. Atmos. Sci*., vol.**55**, no.22, pp.3829–3846, 1999.

[50] A. Numaguchi, S. Sugata, M. Takahashi, T. Nakajima, and

A. Sumi, Study on the climate system and mass transport by a climate model, *CGER's Supercomputer Monograph*, vol.3, Center for Global Environmental Research, National Institute for Environmental Studies, Tsukuba, Japan, 1997.

[51] Fleming, E.L., S. Chandra, J.J. Barnett, and M. Corney, Zonal mean temperature, pressure, zonal wind, and geopotential height as functions of latitude, COSPAR International Reference Atmosphere: 1986, Part II: Middle Atmosphere Models, *Adv. Space Res.*, vol.**10**, no.12, pp.11–59, 1990.

[52] S. Watanabe, K. Sato, and M. Takahashi, A GCM study of orographic gravity waves over Antarctica excited by katabatic winds, submitted to *J. Geophys. Res.*, 2005.